Analysis of Dynamical Processes in a Mouse Visual Decision-Making Task

Stephan Grzelkowski[1], Javier Orlandi[2], and Andrea Benucci[2]

[1] *University of Amsterdam, Amsterdam, Netherlands*
[2] *Riken Center for Brain Science, Wako-shi, Japan*

ABSTRACT

Widefield imaging allows us to simultaneously record multiple areas of the mouse brain. This enables the mapping of the different cortical processes that are involved in the decision-making process. Visual processing is affected by different task modalities, primarily by sensory information and motor components. It is unknown how dorsal-parietal regions separate these overlapping dynamics from visual areas and create relevant representations to make a decision. Using Latent Factor Analysis via Dynamical Systems (LFADS), we analyze the dynamics of widefield neural recordings in a two alternative forced choice orientation discrimination task in mice to find the latent space that encodes relevant information for decision making. We show that LFADS can reliably reproduce the activity of large scale recordings with single-trial precision and that the factor trajectories (the reduced dimensional components) reflect task-related processes. Further analyses of these factors indicate that cortical activity is governed by many behavioral components such as movements, pupil dilation, and task difficulty. We conclude that LFADS offers valuable insights into these interactions and their temporal and spatial dynamics.

Introduction

Decision-making is a complex process as it is affected by many different components. A primary aspect of decision-making is the processing of sensory information.[1,2] However, other aspects of cognition and sensory processing also play an important role, such as the cortical state of the agent[3–5] and sensory-motor transformations.[6] These contributions are reflected in the dynamics of the cortical activity and make it difficult to analyze the neural mechanisms behind the decision-making process.[7]

Both movement and arousal have distinct effects on activity patterns of neurons engaged in visual processing.[8–11] Furthermore, movement related cortical activity carries relevant information to sensory processing. Experiments have shown that knowledge of movements, task-related and non-task-related, improve the accuracy of predicting neural activity.[12] It is unknown how sensory and motor information are separated and interpreted in dorsal-parietal cortices, which engage in the decision-making processes. Neurons in these regions respond to aspects of decision-making and are particularly engaged in the visual sensory processing stream.[13–16] The high-dimensional response space of the activity of early visual processing to sensory and motor related information poses a problem for the downstream interpretation of the signal. The dorsal-parietal regions need to dynamically separate the representations of the sensory and motor information to perform a correct read-out.

Potentially, the read-out is possible because the encoding space of sensory and motor inputs evolve along different dimensions. This would allow the downstream networks to interpret the signal from the sensory areas by making use of the underlying dynamics. To test this hypothesis it is necessary uncover the latent space of both the sensory and the dorsal-parietal areas.

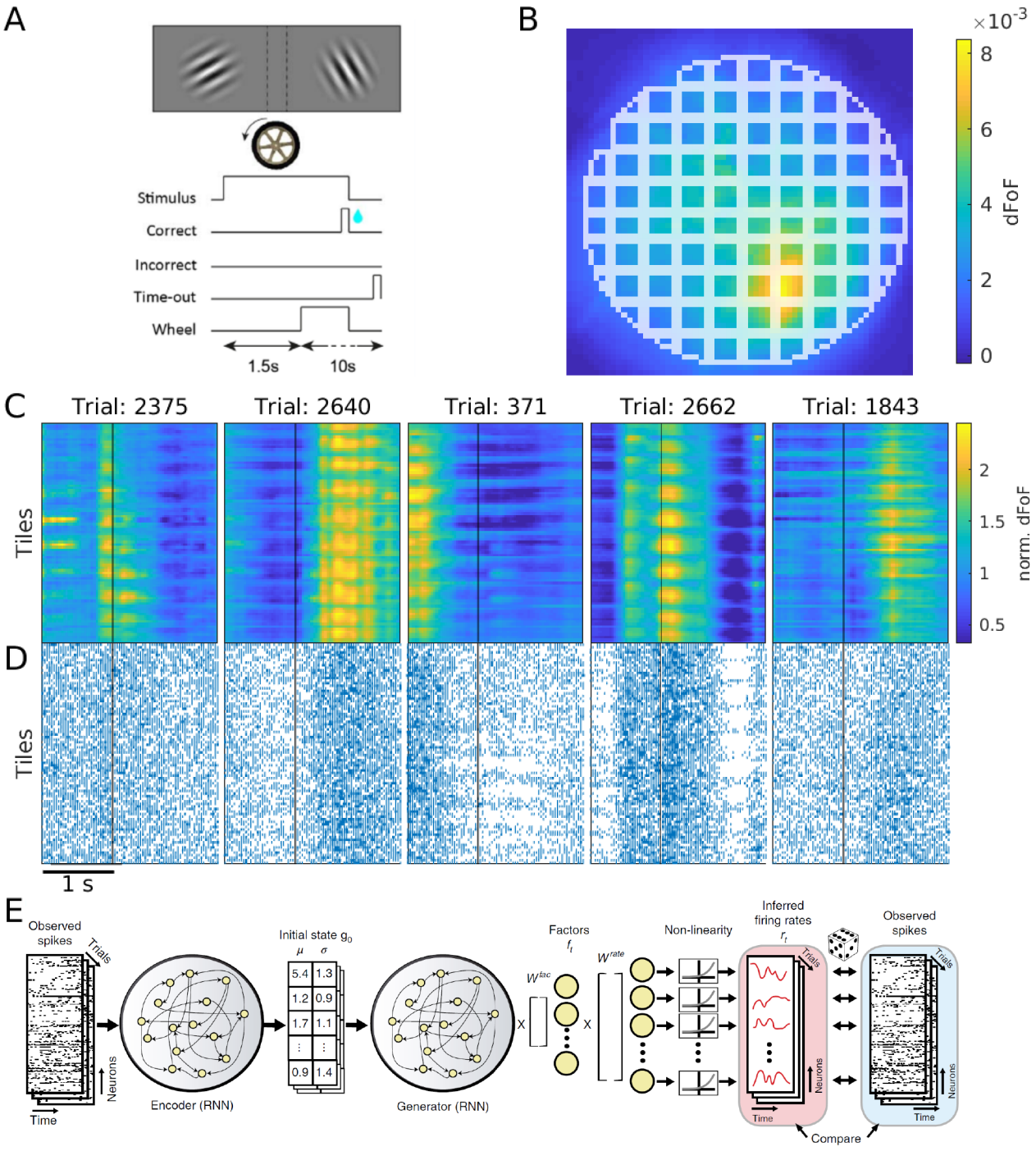

Figure 1: **Task, data generation, LFADS overview. A** Task overview. The upper panel shows an example stimulus. The lower panel shows the timeline of stimulus presentation, the Open Loop period (the first 1.5s), response and reward, and the Closed Loop (up to 10s). Only wheel movement in the Closed Loop period can elicit a reward. **B** An example image of the recorded widefield data averaged over the Open Loop for all trials in one animal. The grid shows the results of the tiling process. The pixels of each tile are averaged to produce the signal that is fed to LFADS (see C). **C** Example heat-plots of tile data in single trials after normalization. The black lines indicate the stimulus onset. **D** Raster plots of the Poisson-generated spike trains in the same trials as C. Black lines indicates stimulus onset. **E** Overview of the LFADS model. Adopted from Pandarinath et al. 2018[17]

Recent developments in the application of Recurrent Neural Networks (RNN's) for neural data analysis allow us to analyze this latent space of cortical network activity.[18] The latent factor analysis of dynamical systems (LFADS), a multi-network stacked non-linear RNN, was able to build low-dimensional representations of the dynamics in macaque motor neurons in an 8-directional reaching task.[17,19,20] The model was able to separate the dynamics for the different reaching directions in the latent space and to reproduce the firing patterns of activated neurons.[17]

Here, we train LFADS to fit the neural dynamics during a two alternative forced choice orientation discrimination task in mice across multiple areas. We apply the model to widefield recordings of multiple areas, including early visual processing and dorsal-parietal networks. This approach makes it possible to analyze the dynamics of visual information processing, motor contributions and decision-making across multiple connected areas. We aim to understand how dorsal-parietal regions make use of different encoding spaces to separate the overlapping representations of different modalities in the sensory areas.

The combination of large scale population recordings and machine learning applications for dynamical systems makes it possible to investigate the dynamics underlying the decision-making process across multiple areas. In this report, we will address the central question: Is LFADS able to uncover a latent space that offers insights into the separation of sensory and motor representations in the dorsal-parietal network for decision-making? We will present the results of training LFADS on Poisson sampled widefield data and an analysis of the dynamics of different task modalities in a two-alternative forced choice orientation discrimination task. We found that LFADS can reproduce the signal with high single-trial accuracy. Furthermore, we investigate the model's ability to isolate the contributions of different task modalities in the low dimensional representations of the data and compare results across animals.

Two alternative forced choice task

The mice (n = 7) were trained in an automated setup[21] to discriminate between orientations of two grating stimuli presented in the left and right visual field (Figure 1 A). They had to evaluate which of the stimuli was closer to a reference orientation, horizontal or vertical (each mouse was trained on one reference). To indicate their choice, the mice moved the stimulus grating into the center of the screen, rotating a wheel in the proper direction. In the first 1.5 s after stimulus onset, the wheel movements did not have an effect on the stimulus position. We termed this period the Open Loop (OL). After the OL, the mice had 10s to move the stimulus to the center of the screen during the Closed Loop (CL). If the target position was not reached the trial was marked as a timeout. The animals reached an average performance of $58.2\%(\pm 11.4\%$ st.dev.) and had an average of $14.4\%(\pm 8.8\%$ st.dev) of timeout trials.

Widefield data & training LFADS

During the task, we measured the wide-field activity through a cranial window that was centered above the right hemisphere towards the dorsal-parietal regions to achieve maximal coverage of the visual processing areas. We successfully brought GCaMP6f to expression in excitatory neurons of the mice. Widefield recordings were acquired under head fixation and the fluorescent activity was measured using a two-lens CMOS camera and a 465 nm excitation LED. (For detailed information on the training and imaging techniques please refer to Abdolrahmani et al.[22]).

We trained LFADS[17] to uncover the dynamics of the decision-making process and to investigate the effects of different task modalities. LFADS is a variational auto-encoder with the task to reproduce the input-rates. It achieves this by minimizing the divergence of the distributions between the input spike rates and the reconstructed rates. LFADS consists of 2 RNN's, the controller network and the generator network (Figure 1E). The controller network has full knowledge of the trial signal. After a forward and backward pass in time of one trial, the activity of the units in the controller networks produce the mean and variance for a gaussian distribution for each unit in the generator network. From these priors, LFADS draws a sample that defines the initial states of the generator units. The generator units evolve at each time point, where the units take inputs only from other units within the network. At each evolution, information from the generator network projects to the factor units. The factor units form the low-dimensional representations of the dynamics in the neural data. A fully connected matrix of weights projects from the factors to units that represent the activity of the tiled cortical maps. The activity goes through a sigmoidal input function and a non-linearity that produces firing rates of the units that represent the tiles in our data.

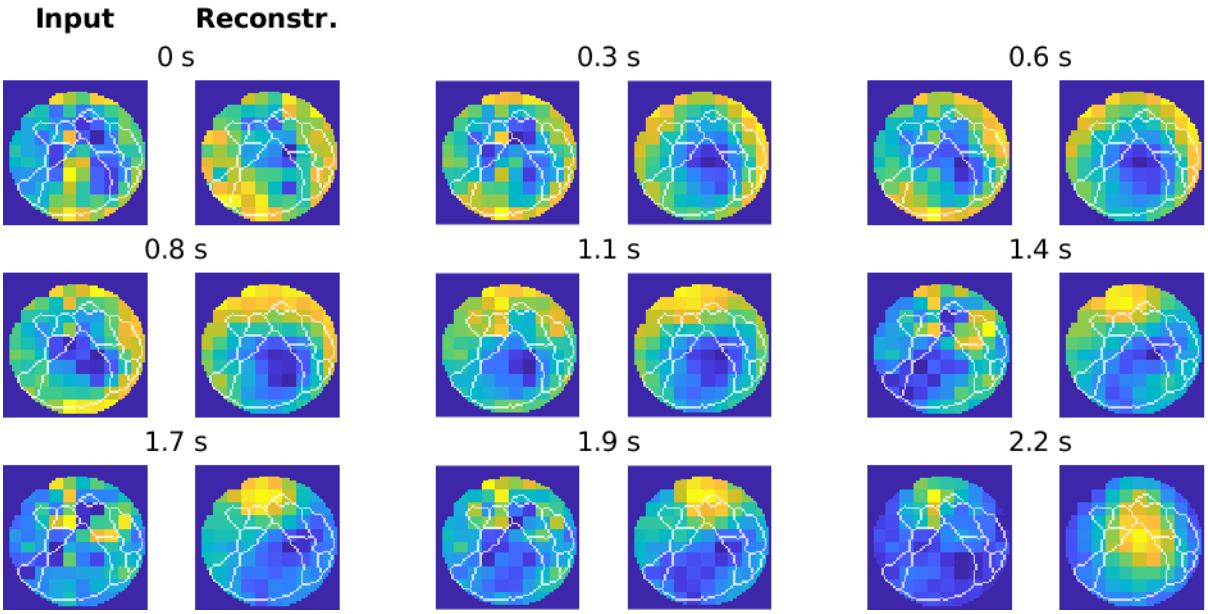

Figure 2: **LFADS reconstruction of the input traces** Comparison of the input rates of the tiles given to LFADS and the Reconstruction by the model. The series of plots spans the OL of one trial. Each set of two plots shows a different time point of the trial. The left plot shows the input and the right plot shows the reconstruction. The white borders indicate the mouse brain areas mapped to the Allen brain atlas.[23]

Optionally, one can sample spikes from these rates to create firing patterns. However, this is unnecessary as we can compare the reconstructed rates to the rates that we used to create the input spike trains. The weights within the 2 RNN's, as well as the connecting weights from input to controller, from controller to generator, from generator to the factors and from the factors to the reconstructed units are trainable. The training consists of adjusting all network weights to minimize the divergence between the reconstructed rates and the input spike trains with a regularizing prior on the distributions of the generator units. For a more detailed explanation of the training process, refer to the two papers from the original authors.[17,19]

Relative to the original framework we had to implement two customizations: (1) the input needed to be constructed of trials of the same lengths and (2) the model was built for spike trains where each input signal was a discrete neural recording. As trials had variable lengths in the CL, we chose to use the signal from 1s before stimulus onset and the full OL period (1.5s) for training. To address the second problem, we tiled the recorded regions into circular area with a 10x10 grid that was chosen manually to avoid the edges of the cranial window (Fig 1B). Along the edges a grid cell was included if at least 40% of its area was covered by the circle. Each tile was treated as a distinct signal. All signals were globally normalized with the following equation:

$$S' = \frac{S - mean(perc[S_T]_5)_{glob}}{mean(max[S_T])_{glob}}$$

where S_T is the averaged signal of one tile, $perc[.]_5$ indicates the lower 5th percentile bound, and $mean(.)_{global}$ indicates the global mean across tiles. This form of normalization was chosen to achieve an appropriate magnitude of variance in the sampled data. We filtered the signal using a 8Hz low-pass filter to avoid high frequency artifacts and noise. From the normalized and filtered data we generated spike trains with a Poisson process, where the probability of λ was given by the rate signal at that time point. As a result, the spike train of a tile could have multiple spikes at a given time-point (Figure 1D). Although this would be an implausible assumption for single-cell recordings with high temporal resolution, it is a reasonable approximation for the widefield data.[24]

Unless otherwise stated, we used 64 units in the controller and generator RNN's, 20 factors and a stop hyperparameter of 0.1×10^{-4} for the training. Other hyperparameters were kept at default (for a full list of hyperparameters see: https://lfads.github.io/lfads-run-

manager/hyperparameters/). The model successfully reproduced the input rates with high precision in single trials with an average explained variance of $86.2\%(\pm 4.4\%$ st.dev.) across animals.

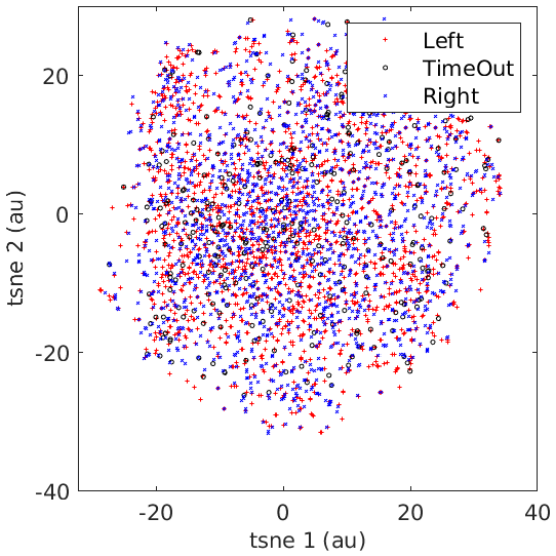

Figure 3: **T-SNE of the generator initial states** This figure shows the t-SNE on the initial states of the generator units. Coloring corresponds to the choice of the animal. Red pluses: left; Black circles: time-out; Blue crosses: right

Analyzing the dynamics of choice

As a first step in the analysis, we investigated different choice conditions: left, right and time-out trials. We performed t-SNE analysis, a method to visualize clustering in high-dimensional data,[25] on the initial states of the generator network units (Figure 3). There was no evidence for clustering in the t-SNE of the initial conditions (Figure 3). Similarly, we did not find significant differences between choice conditions in the factor trajectories (t-test; bonferroni corrected). Our results stand in contrast to findings from training LFADS on the firing patterns of macaque motor neurons during an 8-directional reaching task. There, the 8 directions showed significant differences in the factor trajectories as well as clearly identifiable clustering in the t-SNE of the initial states of the generator units.[17] An explanation for the discrepancy between these two experiments might be found in the higher complexity of the dynamics in the decision-making task. Additionally, it is expected that more components influence the dynamics of the neural activity during the decision-making task compared to the reaching task. To address this, we investigated the factor trajectories under different behavioral conditions and correlating signatures next.

Behavioral condition filtering

To find relevant behavioral conditions for analyzing the dynamics of the factors we carried out a sweep of statistical tests on a broad range of different trial combinations. We selected a set of behavioral parameters:

- **wheel movements**: (1) high (3-10 threshold crossings of wheel velocity in the OL) and (2) low (less than 3 threshold crossings) velocity trials
- **pupil dilation**: (1) low (1st quartile), (2) intermediate (2nd and 3rd quartile) and (3) high (4th quartile) average pupil dilation in the OL
- **task difficulty**: difference between the 2 orientation angles, (1) easy ($> 75°$), (2) intermediate (between $15°$ and $75°$) and (3) difficult ($< 15°$) trials
- **no. of saccades**: (1) no, (2) one or (3) many (more than one) eye movements
- **trial outcome**: was the animal's choice (1) correct or (2) incorrect

We carried out statistical tests comparing the trajectories of the reconstructed rates at each time point for each tile for all possible combinations of trials with more than 20 trials. We analyzed differences between left and right choice trials to find potential dynamics of the decision-making process in the latent space of the factors. A combination of conditions was deemed relevant if at least 10% of its time points showed a significant difference between left and right choice trials (t-test, $p < 0.01$). We summarized the tiles and conditions that were counted relevant in these ways. We found a broad diversity of dependencies, with a strong animal-to-animal variability: 57.1% with dependency on wheel movements, 85.7% with pupil area dependency, 28.6% with dependency on task difficulty, 57.1% with dependency on eye saccades, and 42,9 % with dependency on trial outcome.

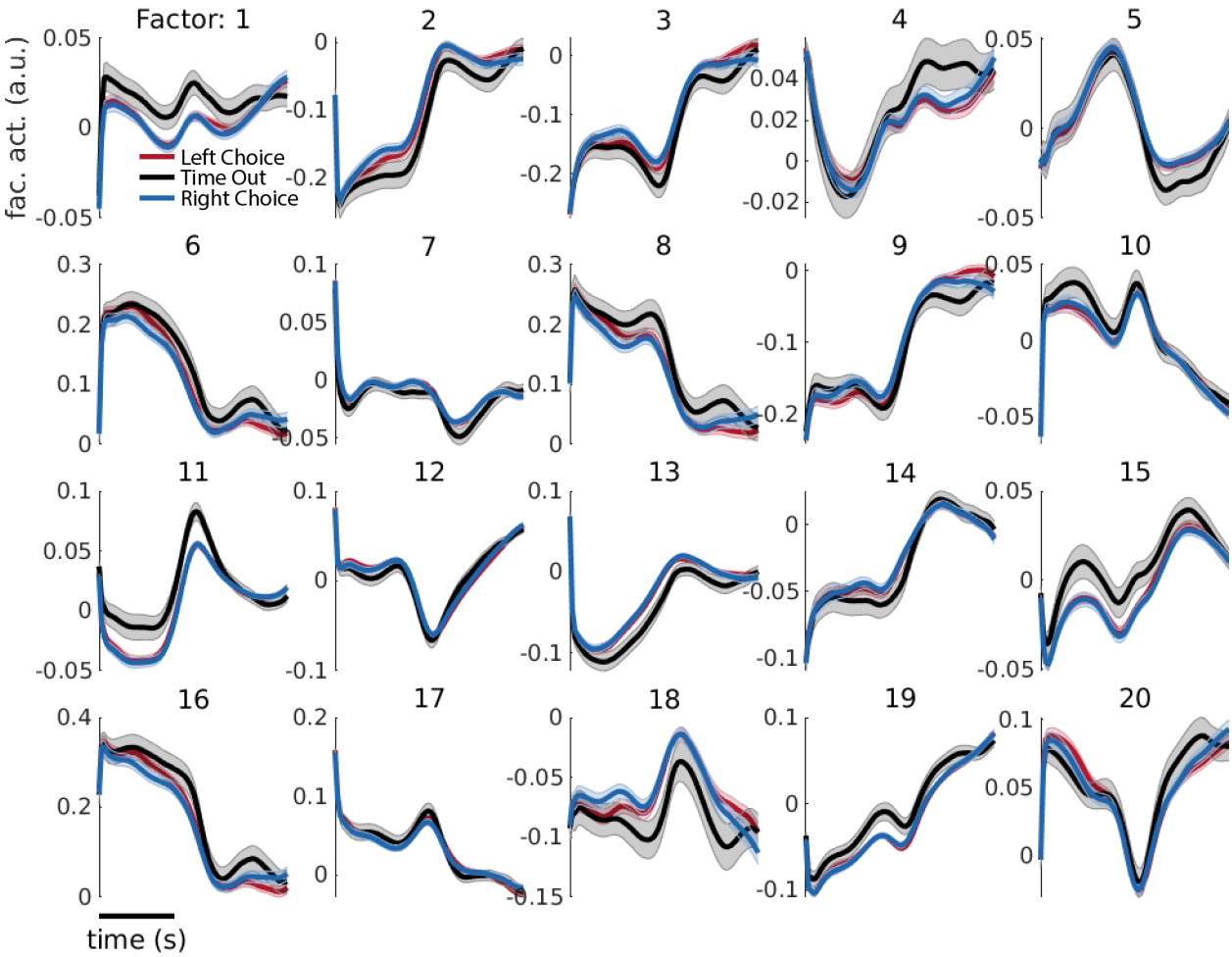

Figure 4: **Factor Traces** Shown here are the factor traces for one animal averaged over all trials with a left choice (Red), right choice (Blue) and time outs (Black).

We further analyzed the connections between the reconstructed rates and the latent space of the factors (Figure 5). It is possible to quantify the factor contributions to different cortical regions through weight maps (Figure 5 B). This could make it possible to investigate the interactions of specific behavioral components to the different areas. However, the high variability across animals makes it difficult to draw conclusions in regards to a shared latent space of the cortical activity during decision-making. Next, we performed angle analysis as another method to find shared features of different behavioral signatures across animals.

Angle analysis

Another way to analyze the contributions of different behavioral signatures to the cortical dynamics is to perform angle analysis.[15,26] As a first step, we computed trial averages of the factor activity for 3 behavioral conditions:

1. pupil area, low vs. high
2. difficulty, small vs. large angle difference
3. wheel movement, high vs. low velocity

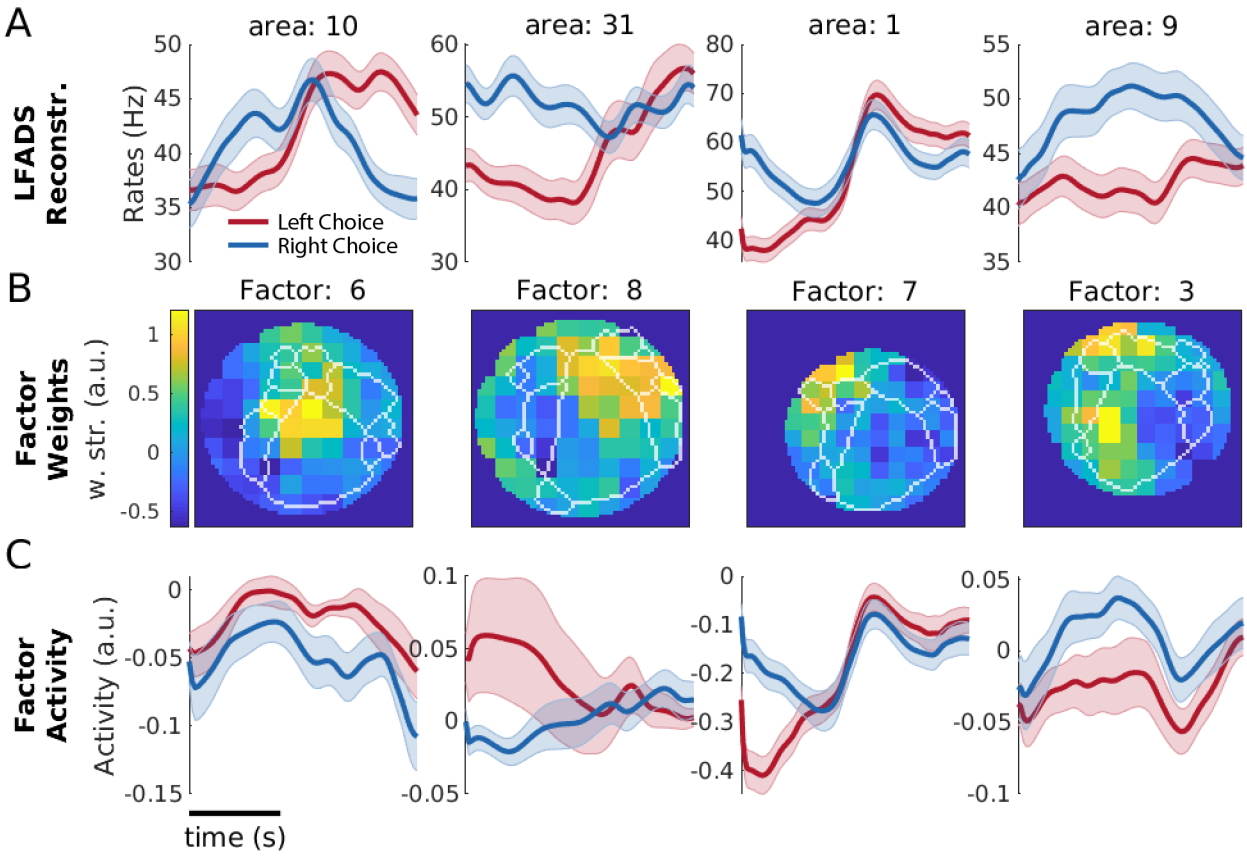

Figure 5: **Rate splits and factor weights.** **A** This panel shows the tiles that had maximal separation averaged for left (red) and right (blue) choice trials under different conditions for 4 of the 7 animals. From left to right: Animal 1, 2, 4, 6. **B** We plot the weight strength from the factor with the strongest connection to the tile depicted in A. **C** The traces of the factors depicted in B averaged over the same trials as in A.

Next, we constructed a projection vector for each combination by computing the angle between the two average vectors of the sub-conditions (e.g. the angle between the average vector of all trials with low pupil area against the average vector of all trials with high pupil area). We used these vectors to project all left and right trials into the dynamic factor space of the 3 listed conditions. Figure 6 shows the 3-dimensional projections onto the behavioral subspaces of the factors. The lines show left (red) and right (blue) projections, where each point on the line corresponds to a time point in the trial and its projection into the angle space for pupil area, difficulty, and wheel movement. Although the trajectory structure bears some resemblance for some animals, e.g. animals 2 and 7, there is generally little consistency. Similarly, a separation between left and right trials is not present in any animals except animal 3.

The high variability in the latent spaces across animals makes it difficult to say conclusively that LFADS is not able to separate the dynamics of different decisions. There are no constraints on the LFADS model that would enforce dynamical structures to hold across different training runs or animals. It is unclear if the different structure of the latent space is a result of individual differences across animals or an aspects of LFADS training process. This hypothesis is testable by separating training runs for different sessions of one animal and repeat the angle analysis to test if the structure holds for all sessions within that animal. Another reason for differences in the dynamical space could be the tiling process. Individual differences in cortical mapping and cranial window coverage could result in large differences in the composition of the input signal given to LFADS. These problems could potentially be solved by creating custom tiles per animal that achieve area coverage according to the Allen brain atlas.[23]

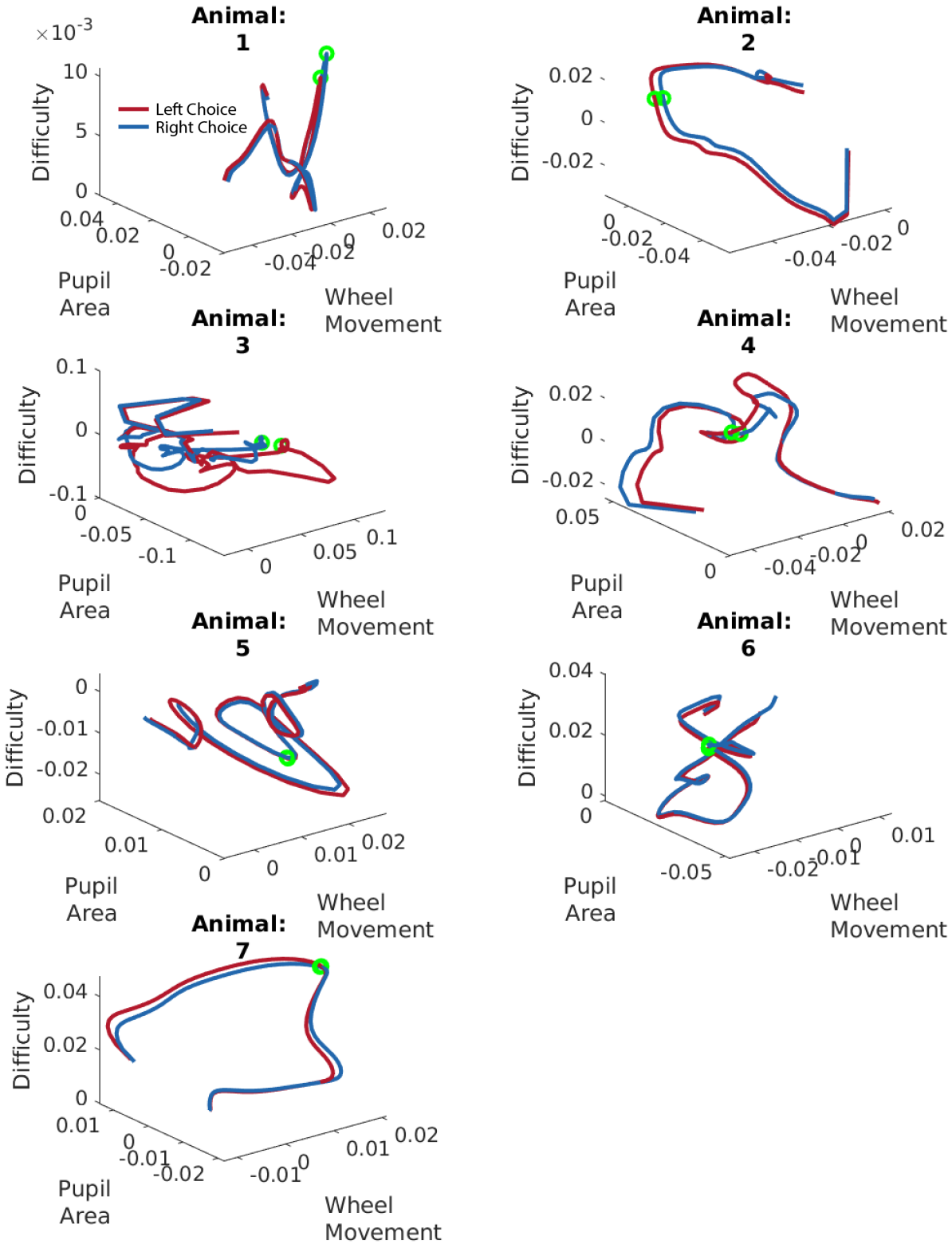

Figure 6: **Angle analysis individual animals** We plotted the projection of left (red) and right (blue) trials onto the vector space of the wheel movement, pupil area and difficulty (see methods). The traces evolve through the time of the trial. The green dots represent trial start.

Drawbacks & future plans

There are some drawbacks with the presented analyses that were not addressed due to time limitations. We did not exclude sessions that had low performance or a large percentage of time-out trials. As a result, the analyses might include trials in which animals were inattentive to the task. As the cortical state depends on the attentive state of an animal,[27,28] this might negatively affect LFADS' ability to find the relevant latent space for decision making. We plan to repeat the LFADS training and the analyses excluding sessions with a low performance and sessions with a high rate of time-out trials.

Furthermore, the approach we took to identify relevant behavioral conditions by ordering them by percentage of significant t-test results is likely not reliable. There are two ways to address this issue. We could carry out separate analysis to identify quantitatively the behavioral signatures that maximally shape the latent space. A literature search could be another valuable method to determine qualitatively which conditions are candidates for further investigation. Although we considered evidence on the effects of pupil dilation and wheel movement on neural population dynamics,[6–8,29] other task modalities were analyzed with less care, such as task difficulty, where similar effects have been found in dorsal-parietal regions.[30,31]

Trial outcome, correct vs. incorrect trials, also seemed to greatly affect the latent space of the LFADS representations. As differences between these trials are unlikely to be a result of reward related effects, which would be expected to arise at a later time point (around reward delivery) and in frontal regions,[32,33] we want to further investigate this subspace.

Discussion

We have shown that the LFADS model is able to reconstruct the activity patterns in widefield data of multiple areas in a complex decision task with high single-trial accuracy. This opens up a wide range of possible applications for the algorithm. In contrast to earlier research, that showed separation in the latent spaces of M1 neuronal activity in a macaque reaching task,[17] it proved difficult to find meaningful boundaries in the dynamics between different choices made by the animal. We did not see significant clustering in the t-SNE analysis on the initial generator states (Figure 3) or in a crude analysis of the factor trajectories between left and right trials (Figure 4). An explanation for this discrepancy might be the increased complexity in both the behavioral and the cortical components in decision-making compared to the reaching task.

To address this, we created subsets of trials with different behavioral signatures of difficulty, pupil area, wheel movements, trial difficulty, and saccades. We compared left and right choice trials in these combinatorial spaces to find relevant behavioral markers for the cortical dynamics of decision making. Although we found that this method succeeded at indicating relevant behavioral markers and areas for further investigation, there was little consistency across animals. Nonetheless, the factor trajectories under these constrained conditions seem a promising candidate for analyzing the latent space of decision-making. We expect that an analysis of the factor projections, i.e. the weight maps (Figure 5 B), will offer great insights into the workings of the cortical mechanisms as a valuable tool for analyzing the spatial and temporal components.

The projections in the angle analysis of left and right trials onto the differential vector spaces of the most prominent behavioral separators did not show high coherence across different animals. From all results taken together, we must conclude that LFADS is not suitable to find consistent dynamics across animals as it has trouble accounting for individual differences. Nonetheless, we believe that we have not exhausted to possibility space of the model to investigate the latent space of decision-making. Specifically, an analysis of the temporal components of the factor dynamics and their projections onto the cortical map could provide insights into the separation of motor and sensory components that takes place in the dorsal-parietal regions.

A complication that needs to be addressed in future experiments is the ambiguity of the decision point in a trial. After the fixed time of the OL, there is a variable time window in which the animal is allowed to make a correct response to receive a reward. As a result, it is difficult to determine a time-point at which the animal makes its decision. Hence, it is challenging to extract the relevant cortical signatures that relate to the decision-making process. We considered a solution to this, where we construct inputs that have a set trial interval with a time window that reverses from the time-point of the pivotal wheel movement. A problem with this approach is that the ambiguity remains as the decision might not be locked to the movement onset, e.g. a decision could have been reached in the OL segment. This points to a problem in decision-making research, as the temporal aspects of this process are poorly un-

derstood.[34] However, LFADS could help solve this issue, as with the right task setup and training regime it might be possible to deconstruct the latent space of the cortical activity through the factors. If we could map the connections between the features of the latent space and behavioral components it should be possible find correlates of decision making.

The experimental results of the LFADS application to motor neurons has found widespread interest in the community of Brain Computer Interface (BCI) research. Using the latent space representations as a way of classifying motor sequences is expected to yield improvements for BCI decoders.[35–37] Expanding LFADS' ability to uncover the latent space of higher cognitive functions, like decision making, could potentially expand the capabilities of BCI. We expect that LFADS will prove a useful tool for the analysis of cortical dynamics and find many other applications.

References

1. Alan E Rorie, Juan Gao, James L McClelland, and William T Newsome. Integration of sensory and reward information during perceptual decision-making in lateral intraparietal cortex (lip) of the macaque monkey. *PloS one*, 5(2):e9308, 2010.
2. Joshua I Gold and Michael N Shadlen. Neural computations that underlie decisions about sensory stimuli. *Trends in cognitive sciences*, 5(1):10–16, 2001.
3. Christian R Lee and David J Margolis. Pupil dynamics reflect behavioral choice and learning in a go/nogo tactile decision-making task in mice. *Frontiers in behavioral neuroscience*, 10:200, 2016.
4. Peter R Murphy, Joachim Vandekerckhove, and Sander Nieuwenhuis. Pupil-linked arousal determines variability in perceptual decision making. *PLoS computational biology*, 10(9):e1003854, 2014.
5. Eugene F Civillico and Diego Contreras. Spatiotemporal properties of sensory responses in vivo are strongly dependent on network context. *Frontiers in systems neuroscience*, 6:25, 2012.
6. Julia Trommershäuser, Laurence T Maloney, and Michael S Landy. Decision making, movement planning and statistical decision theory. *Trends in cognitive sciences*, 12(8):291–297, 2008.
7. Xiao-Jing Wang. Neural dynamics and circuit mechanisms of decision-making. *Current opinion in neurobiology*, 22(6):1039–1046, 2012.
8. Martin Vinck, Renata Batista-Brito, Ulf Knoblich, and Jessica A Cardin. Arousal and locomotion make distinct contributions to cortical activity patterns and visual encoding. *Neuron*, 86(3):740–754, 2015.
9. Matthew J McGinley, Martin Vinck, Jacob Reimer, Renata Batista-Brito, Edward Zagha, Cathryn R Cadwell, Andreas S Tolias, Jessica A Cardin, and David A McCormick. Waking state: rapid variations modulate neural and behavioral responses. *Neuron*, 87(6):1143–1161, 2015.
10. Daisuke Shimaoka, Kenneth D Harris, and Matteo Carandini. Effects of arousal on mouse sensory cortex depend on modality. *Cell reports*, 22(12):3160–3167, 2018.
11. Corbett Bennett, Sergio Arroyo, and Shaul Hestrin. Subthreshold mechanisms underlying state-dependent modulation of visual responses. *Neuron*, 80(2):350–357, 2013.
12. Simon Musall, Matthew T Kaufman, Ashley L Juavinett, Steven Gluf, and Anne K Churchland. Single-trial neural dynamics are dominated by richly varied movements. *bioRxiv*, page 308288, 2019.
13. Dmitry Lyamzin and Andrea Benucci. The mouse posterior parietal cortex: anatomy and functions. *Neuroscience research*, 2018.
14. Gerald N Pho, Michael J Goard, Jonathan Woodson, Benjamin Crawford, and Mriganka Sur. Task-dependent representations of stimulus and choice in mouse parietal cortex. *Nature communications*, 9(1):2596, 2018.
15. Christopher D Harvey, Philip Coen, and David W Tank. Choice-specific sequences in parietal cortex during a virtual-navigation decision task. *Nature*, 484(7392):62, 2012.
16. Michael Krumin, Julie J Lee, Kenneth D Harris, and Matteo Carandini. Decision and navigation in mouse parietal cortex. *ELife*, 7:e42583, 2018.
17. Chethan Pandarinath, Daniel J O'Shea, Jasmine Collins, Rafal Jozefowicz, Sergey D Stavisky, Jonathan C Kao, Eric M Trautmann, Matthew T Kaufman, Stephen I Ryu, Leigh R Hochberg, et al. Inferring single-trial neural population dynamics using sequential auto-encoders. *Nature methods*, page 1, 2018.

18. M Yu Byron, Afsheen Afshar, Gopal Santhanam, Stephen I Ryu, Krishna V Shenoy, and Maneesh Sahani. Extracting dynamical structure embedded in neural activity. In *Advances in neural information processing systems*, pages 1545–1552, 2006.

19. David Sussillo, Rafal Jozefowicz, LF Abbott, and Chethan Pandarinath. Lfads-latent factor analysis via dynamical systems. *arXiv preprint arXiv:1608.06315*, 2016.

20. Chethan Pandarinath, Jasmine Collins, Rafal Jozefowicz, Sergey Stavisky, Jonathan Kao, Mark Churchland, Matt Kaufman, Stephen Ryu, John Henderson, Krishna Shenoy, et al. Precise estimates of single-trial dynamics in motor cortex using deep learning techniques. 2017.

21. Ryo Aoki, Tadashi Tsubota, Yuki Goya, and Andrea Benucci. An automated platform for high-throughput mouse behavior and physiology with voluntary head-fixation. *Nature communications*, 8(1):1196, 2017.

22. Mohammad Abdolrahmani, Dmitry R Lyamzin, Ryo Aoki, and Andrea Benucci. Cognitive modulation of interacting corollary discharges in the visual cortex. *bioRxiv*, page 615229, 2019.

23. Hong Wei Dong. *The Allen reference atlas: A digital color brain atlas of the C57Bl/6J male mouse.* John Wiley & Sons Inc, 2008.

24. Jason R Swedlow and Melpomeni Platani. Live cell imaging using wide-field microscopy and deconvolution. *Cell structure and function*, 27(5):335–341, 2002.

25. Laurens van der Maaten and Geoffrey Hinton. Visualizing data using t-sne. *Journal of machine learning research*, 9(Nov):2579–2605, 2008.

26. Nuo Li, Kayvon Daie, Karel Svoboda, and Shaul Druckmann. Robust neuronal dynamics in premotor cortex during motor planning. *Nature*, 532(7600):459, 2016.

27. Kenneth D Harris and Alexander Thiele. Cortical state and attention. *Nature reviews neuroscience*, 12(9):509, 2011.

28. Marieke L Schölvinck, Aman B Saleem, Andrea Benucci, Kenneth D Harris, and Matteo Carandini. Cortical state determines global variability and correlations in visual cortex. *Journal of Neuroscience*, 35(1):170–178, 2015.

29. Jacob Reimer, Emmanouil Froudarakis, Cathryn R Cadwell, Dimitri Yatsenko, George H Denfield, and Andreas S Tolias. Pupil fluctuations track fast switching of cortical states during quiet wakefulness. *Neuron*, 84(2):355–362, 2014.

30. A Assmus, JC Marshall, J Noth, K Zilles, and GR Fink. Difficulty of perceptual spatiotemporal integration modulates the neural activity of left inferior parietal cortex. *Neuroscience*, 132(4):923–927, 2005.

31. Marios G Philiastides, Roger Ratcliff, and Paul Sajda. Neural representation of task difficulty and decision making during perceptual categorization: a timing diagram. *Journal of Neuroscience*, 26(35):8965–8975, 2006.

32. Masataka Watanabe. Reward expectancy in primate prefrental neurons. *Nature*, 382(6592):629, 1996.

33. Peter C Holland and Michela Gallagher. Amygdala–frontal interactions and reward expectancy. *Current opinion in neurobiology*, 14(2):148–155, 2004.

34. Alexander C Huk and Michael N Shadlen. Neural activity in macaque parietal cortex reflects temporal integration of visual motion signals during perceptual decision making. *Journal of Neuroscience*, 25(45):10420–10436, 2005.

35. Aaron P Batista and James J DiCarlo. Deep learning reaches the motor system. *Nature methods*, 15(10):772, 2018.

36. Chethan Pandarinath, K Cora Ames, Abigail A Russo, Ali Farshchian, Lee E Miller, Eva L Dyer, and Jonathan C Kao. Latent factors and dynamics in motor cortex and their application to brain–machine interfaces. *Journal of Neuroscience*, 38(44):9390–9401, 2018.

37. Ta-Chu Kao and Guillaume Hennequin. Neuroscience out of control: control-theoretic perspectives on neural circuit dynamics. *Current Opinion in Neurobiology*, 58:122–129, 2019.